Crossover from $S=1/2$ to $S=1$ Haldane state in the ferromagnetic and antiferromagnetic alternating Heisenberg chain system $(CH_3)_2CHNH_3CuCl_3$ observed with EPR at 24 GHz

H. Manaka* and I. Yamada
Department of Physics, Faculty of Science, Chiba University, Yayoi-cho, Inage-ku, Chiba 263-8522, Japan
(Received 29 March 2000; revised manuscript received 19 June 2000)

The compound $(CH_3)_2CHNH_3CuCl_3$, which consists of ferromagnetic-dominant ferromagnetic and antiferromagnetic alternating Heisenberg chains with $S=1/2$, is regarded as a Haldane system with $S=1$ at low temperatures because a pair of ferromagnetically coupled spins behaves as $S=1$. There should therefore be a crossover of the spin state from $S=1/2$ to $S=1$ when the temperature is decreased. With the expectation that the crossover causes a drastic change in spin dynamics, electron paramagnetic resonance (EPR) experiments were performed at 24 GHz on single crystals of this compound over the region of 1.4–295 K. The EPR spectra observed below 10 K were found to show characteristics clearly distinct from those above 10 K. That is, a single absorption line observed above 10 K was found to split into two lines below 10 K, and an additional weak line appeared at a position corresponding to half of the averaged resonance fields of the two lines. The resonance fields of the two lines vary with the direction of the external field H; their angular dependence is $a \pm b(1-3\cos^2\theta)$, where a and b are constants, and θ is the angle between the direction of H and one of the normals of the orthogonal crystal surfaces. The resonance field of the weak line that appeared at the half-field position was almost constant with respect to the direction of H. These experimental results observed below 10 K are explained when one considers that the $S=1$ state caused by pairs of ferromagnetically coupled two spins supersedes the $S=1/2$ state of the individual spins. Then the dipole–dipole interaction ($\mathcal{H}'_{DD}$) and the anisotropic exchange interaction ($\mathcal{H}'_{AE}$) between ferromagnetically coupled two spins act as a fictitious single ion anisotropy, and remove the threefold degeneracy of the triplet state of $S=1$, i.e., $E_{S,S_z}=E_{1,1}, E_{1,0}$, and $E_{1,-1}$. As a result, the $\Delta S_z=\pm 1$ transitions, i.e., the transitions between $E_{1,-1}$ and $E_{1,0}$, and between $E_{1,0}$ and $E_{1,1}$ bring about two absorption lines. That is why the two lines appear below 10 K. The weak half-field line is due to the $\Delta S_z=\pm 2$ transition, which is also caused by $\mathcal{H}'_{DD}$ and $\mathcal{H}'_{AE}$ between ferromagnetically coupled two spins because nondiagonal elements between $|1,1\rangle$ and $|1,-1\rangle$ are not 0.

I. INTRODUCTION

Ferromagnetic and antiferromagnetic (F–AF) alternating Heisenberg chains with $S=1/2$ can be regarded as Haldane systems with $S=1$ (Ref. 1) when the ferromagnetic exchange interaction is much stronger than the antiferromagnetic one.[2,3] That is, an energy gap between the singlet ground state and the triplet excited state is expected at $T=0$ K. In such a system, spins behave as 1/2 at high T where no magnetic short-range order exists, whereas they are expected to behave as $S=1$ when T decreases and spin correlations develop. How does spin dynamics (or spin relaxation phenomena) change when T decreases from the region of $S=1/2$ to that of $S=1$? This question led us to perform electron paramagnetic resonance (EPR) experiments on an ideal F–AF Heisenberg chain system.

The compound $(CH_3)_2CHNH_3CuCl_3$ (abbreviated as $IPACuCl_3$) was recently found to be an ideal model of such a F–AF system.[4] The magnetic chain formed in this compound is shown in Fig. 1. Two Cu ions comprising a pair are in the same plane and these pairs are piled up stepwise. The two Cu ions in each plane are bibridged via Cl_1 and Cl_1', while those located in the adjacent planes are bibridged via Cl_2 and Cl_2^*. So, there are two kinds of exchange interactions. Since each magnetic chain is separated by nonmagnetic radicals such as $(CH_3)_2CH$ and NH_3, the magnetic one dimensionality of this compound is excellent.

As reported in Ref. 4, for the three directions of an external field H parallel to the normals of the flat orthogonal surfaces of an as-grown single crystal, each $\chi(T)$ curve shows a round peak around 24 K ($\equiv T_{max}$) and monotonically decreases to zero, as shown in Fig. 2. This indicates that, with decreasing T, spin correlations increase, and then

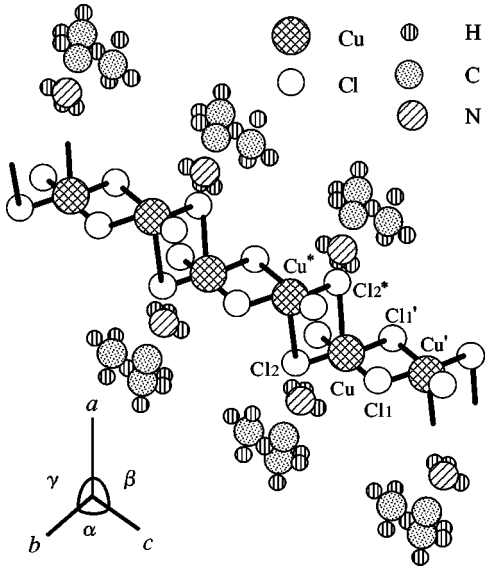

FIG. 1. Crystal structure of $(CH_3)_2CHNH_3CuCl_3$.

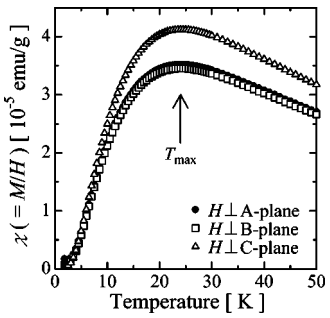

FIG. 2. The temperature dependence of the magnetic susceptibility $\chi(T)$ observed at $H=100$ Oe. The direction of the external field is perpendicular to the three orthogonal surfaces of an as-grown sample, A, B, and C, respectively. $\chi(T)$ reaches its maximum at 24 K $\equiv T_{\max}$.

ferromagnetically coupled spin pairs that behave as spins with $S=1$ are created below $T_{\max}$. As a result, the singlet and the triplet energy levels are formed, and the population of spins on the singlet ground state increases when T decreases to 0 K, which results in the decrease in $\chi(T)$ to 0.

On the basis of the $\chi(T)$ data, the alternated exchange interactions were determined to be $J_F/k=+54.1$ K and $J_{AF}/k=-23.5$ K,[4] where the two exchange interactions are defined in a Hamiltonian

$$\mathcal{H}=-2J_{AF}\sum_{i=1}^{N/2}\mathbf{S}_{2i}\cdot\mathbf{S}_{2i+1}-2J_F\sum_{i=1}^{N/2}\mathbf{S}_{2i}\cdot\mathbf{S}_{2i-1}. \quad (1.1)$$

The energy gap Δ between the singlet and the triplet state was also estimated from $\chi(T)$ to be $\Delta/k\simeq 17.5$ K $=13.0$ T for $g=2.00$.[4] To directly confirm the existence of the energy gap in this compound, measurements of the magnetization process at low T were also made, and a value Δ, which was consistent with that given above, was obtained.[5] In H, the triplet splits and the lowest component crosses the singlet at a certain field. Above that field, the interchain exchange interaction, if it exists, would lead to the magnetic long-range order at a finite temperature. According to the specific heat measurements in H, the magnetic long-range order was found for H above about 10 T which corresponds to Δ.[6]

Considering the results of experiments and analyses roughly reviewed above, we thought that $IPACuCl_3$ could be a good candidate to clarify the answer to the question introduced earlier, i.e., How does the spin dynamics change with decreasing temperature from $S=1/2$ to $S=1$? Among several experimental methods applied in an effort to elucidate the answer to this question, we first performed EPR experiments. We found that the characteristics of exchange-narrowed EPR line drastically changed around 10 K. That is, the single absorption line split into two lines below 10 K, and a weak line appeared at a position corresponding to half of the averaged values of the two lines. These findings strongly suggest a crossover from the $S=1/2$ state to the $S=1$ state. After showing the experimental results in the next section, we analyze them successively.

II. EXPERIMENTAL RESULTS

EPR measurements were performed on single crystals using a conventional 100 kHz field-modulated K-band spectrometer with a cavity of TE_{011} mode operated at 24 GHz. Since this compound undergoes a structural transition at 50° C,[4,7] and the F–AF alternation is not assured above 50 °C, we restricted our measurements to temperatures below room temperature. The cavity, with a mechanism for sample rotation around the vertical axis, was inserted in a liquid-He cryostat with electronic temperature control, which made it easy to obtain data on angular dependence and temperature dependence. Absorption spectra observed at various temperatures over the temperature region of 1.4–295 K were traced as derivative lines. Since no cleavage planes parallel to the crystal axes were found, probably due to the triclinic crystal structure, an external field H was applied along the normals of the three orthogonal surfaces of each as-grown sample, A, B, and C, as named in Ref. 4. The direction of magnetic chains is nearly parallel to the normal of the A plane. To measure the angular dependence of the EPR line, the direction of H is rotated in the three planes, each of which involves two normals among the three of the A, B, and C plane.

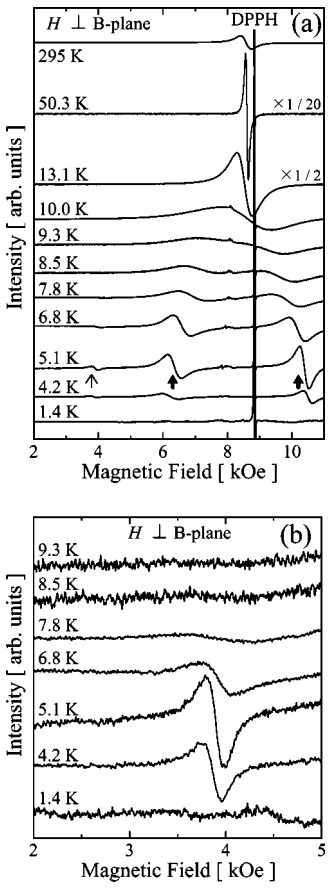

FIG. 3. (a) The EPR spectra obtained at 24.5 GHz for various temperatures below 295 K. The direction of the external field H is perpendicular to the B plane. Bold arrows indicate two lines appearing below about 10 K, and a thin arrow indicates the half-field line. (b) The lower field part of (a) is shown on an expanded scale. The half-field line appearing below 10 K is shown.

Figure 3(a) shows several examples of EPR spectra observed below 295 K for $H\perp$ B plane. At 295 K, which is high enough compared with J_F/k and $|J_{AF}|/k$, a single EPR line appears. The line shapes for $H\perp$ A, B, and C plane were examined at 295 K, and were found to be Lorentzian for the

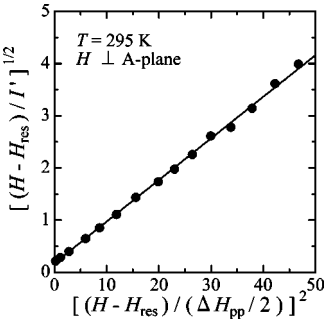

FIG. 4. Analysis of the line shape observed at 295 K for $H\perp$ A plane; this direction of H is nearly along the magnetic chains. The solid straight line corresponds to a Lorentzian line shape. I' is the height of the derivative line.

three directions of H. An example of the analysis of line shape is shown in Fig. 4.

As can be seen in Fig. 3(a), the single line persists down to 10 K with its width varying with T, whereas two lines appear in the spectra obtained below 8.5 K, as indicated by two bold arrows. Moreover, a weak line is seen at a lower field in the spectra observed at 6.8, 5.1, and 4.2 K, as indicated by a thin arrow. The variation of the weak line with T is expanded in Fig. 3(b). Since the resonance field of this weak line is nearly half of the averaged fields of the two lines, we call it a half-field line. For $H\perp$ A and C plane, the temperature dependence of the spectra was similar to that observed for $H\perp$ B plane.

We now show the temperature dependence and the angular dependence of the respective factors of the observed EPR lines, such as the peak-to-peak derivative linewidth $\Delta H_{\rm pp}$, the resonance field $H_{\rm res}$ and the absorption intensity. The value of $\Delta H_{\rm pp}$ at 295 K varies from 300 to 500 Oe with the change in direction of H. Since the principal axes of the crystal did not coincide with the normals of the three surfaces of the sample, the observed angular dependence of $\Delta H_{\rm pp}$ was not simple, and no useful result was obtained from the analysis of it. We therefore omit showing it.

Figure 5(a) shows the changes in $\Delta H_{\rm pp}(T)$ obtained for $H\perp$ A, B, and C plane. For these three directions of H, $\Delta H_{\rm pp}(T)$ shows similar behavior in each instance; with decreasing T, a gradual decrease in $\Delta H_{\rm pp}(T)$ is observed, reaching a minimum at around 50 K, and thereafter the values begin to increase and diverge around 10 K. The rate of increase is prominent below 24 K$\equiv T_{\rm max}$ at which $\chi(T)$ reaches its maximum, as can be seen in Fig. 5(b), which is an expansion of the lower temperature part of Fig. 5(a). Below 10 K, $\Delta H_{\rm pp}(T)$ rapidly decreases with further decreasing T.

The T dependence of the resonance field $H_{\rm res}$ of the single line observed above 10 K is shown in Fig. 6(a). In this figure, the value of $H_{\rm res}(T)-H_{\rm res}(295\ {\rm K})$ is plotted as a function of T. When T decreases from 295 K, $H_{\rm res}$ for the three directions of H remains constant down to a temperature corresponding to $T_{\rm max}$, and then the values begin to shift to the lower or higher field side depending on the direction of H with further decreasing T to 10 K. The g values determined from $H_{\rm res}$ at 295 K for $H\perp$ A, B, and C plane are $g_{\rm A}=2.11$, $g_{\rm B}=2.06$, and $g_{\rm C}=2.25$, respectively.

The resonance fields of the two lines, that appear below 10 K, show remarkable shifts with decreasing T, as shown in Fig. 6(b); the two lines shift oppositely irrespective of the direction of H. In contrast, the position of the half-field line is almost independent of T, as shown also in Fig. 6(b). With respect to the angular dependence of $H_{\rm res}$ of the two lines observed at 4.2 K, as shown in Fig. 7, the $H_{\rm res}$ values well fit the curves expressed by the equation $a\pm b(1-3\cos^2\theta)$, where a and b are constants, and θ is the angle between the direction of H and the normal of the B plane.

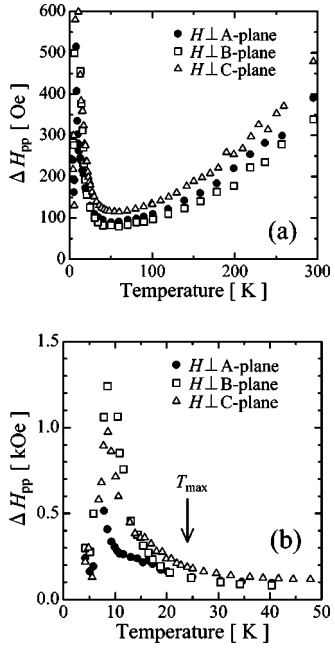

FIG. 5. (a) The temperature dependence of the derivative peak-to-peak linewidth $\Delta H_{\rm pp}$ for an external field applied perpendicular to the A, B, and C planes, respectively. At 295 K, $\Delta H_{\rm pp}=300\sim500$ Oe. (b) The lower temperature part of (a). $\Delta H_{\rm pp}(T)$ for the three directions of H rapidly increases below 24 K $\equiv T_{\rm max}$ at which $\chi(T)$ reaches its maximum, and the values seem to diverge around 10 K. Below 10 K, $\Delta H_{\rm pp}(T)$ of one of the two lines, i.e., the one that appears at a higher field, is plotted. $\Delta H_{\rm pp}(T)$ of the lower field is similar to that of the higher field.

The T dependence of the absorption intensity at low temperatures is given in Fig. 8. Since similar results were obtained for $H\perp$ A, B, and C plane, only the result for $\perp$ B plane is shown. Below 10 K, the absorption intensity means the sum of the intensity of the two lines. As can be seen Fig. 8, there is no anomaly around 10 K within the accuracy of this experiment and the intensity tends to approach zero with decreasing T.

The angular variation of the half-field line observed at 4.2 K is shown in Fig. 9(a). As can be seen in this figure, the derivative peak-to-peak height rapidly decreases when θ approaches 0°, whereas $\Delta H_{\rm pp}$ is almost angular independent. The absorption intensity has consequently a strong angular dependence, as shown in Fig. 9(b). That is, the half-field line disappears when $\theta=0°$, i.e., $H\perp$ B plane, and its intensity increases when θ approaches 90°.

III. ANALYSIS AND DISCUSSION

In spite of the absence of a magnetic long-range order at finite temperatures under H lower than about $10T$,[6] the characteristics of the EPR line observed at 24 GHz drastically

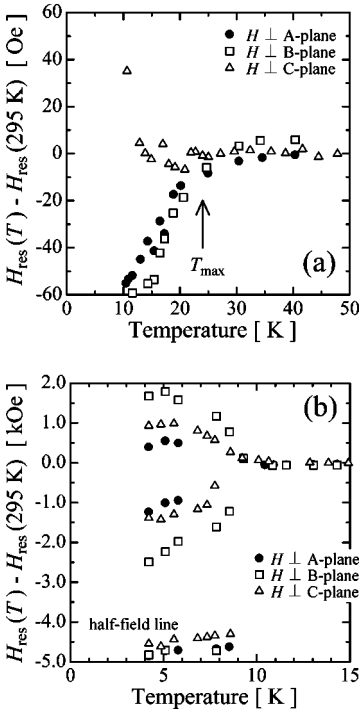

FIG. 6. (a) The temperature dependence of the resonance field $H_{\rm res}(T)$ above 10 K. The values of $H_{\rm res}(T)-H_{\rm res}(295\ {\rm K})$ are plotted, where $H_{\rm res}(295\ {\rm K})$ is the resonance field at 295 K. The g values determined from $H_{\rm res}$ at 295 K are $g_{\rm A}=2.11$, $g_{\rm B}=2.06$, and $g_{\rm C}=2.25$. (b) The temperature dependence of the resonance fields of the two lines and the half-field line.

change around 10 K, as demonstrated in the preceding section. That is, $\Delta H_{\rm pp}(T)$ shows a divergence and $H_{\rm res}(T)$ shifts from that at high temperatures when T decreases to 10 K, as if a magnetic phase transition occurs at 10 K. Moreover, instead of the single line observed above 10 K, two lines appear below 10 K accompanied by an additional weak half-field line. As will be explained later, the anomalous behavior of the EPR line around 10 K is evidence of the crossover of the spin state from $S=1/2$ to $S=1$. We therefore discuss the experimental results obtained above 10 K separately from those below 10 K.

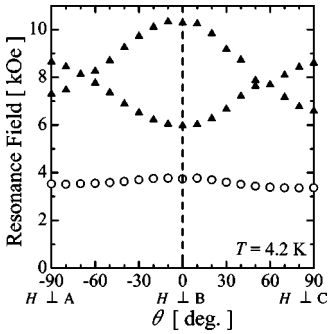

FIG. 7. The angular dependence of the resonance fields of the two lines and the half-field line observed at 4.2 K. The resonance fields of the two lines are shown by closed triangles, while that of the half-field line is shown by open circles. The resonance fields of the two lines obey the relations expressed by the equation $H_{\rm res}\simeq a \pm b(1-3\cos^2\theta)$, where θ is the angle between the direction of H and the normal of the B plane.

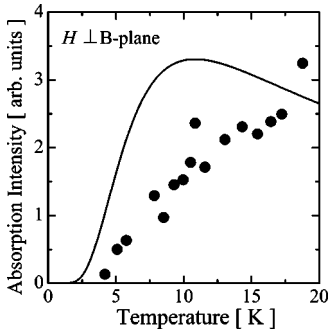

FIG. 8. The temperature dependence of the absorption intensity. The closed circles above 10 K represent the intensity of the single line, whereas those below 10 K represent the sum of the intensities of the two lines. Since the data obtained for the three directions of H are similar, only the data for $H\perp$ B plane are shown. We find no anomaly around 10 K within the accuracy of the experiment. The solid line is a theoretical curve obtained using Eqs. (3.4) and (3.5) with $D^*/g(0)\mu_{\rm B}=-2.2$ kOe, $H_{\rm H}=10.7$ kOe, $H_{\rm L}=6.3$ kOe, $g(0)=2.06$, and $\Delta/k=17.5$ K.

A. Above 10 K; the $S=1/2$ state

At high temperatures that satisfy $T\gg J_{\rm F}/k$, $|J_{\rm AF}|/k$, the spins in this compound behave as $S=1/2$ because the spin correlation is absent or very weak. We first clarify perturbation terms that cause broadening of the EPR line of this compound. According to the crystal symmetry reported in Refs. 4 and 7, a center of inversion exists between Cu and Cu′, and also between Cu and Cu* (see Fig. 1), indicating

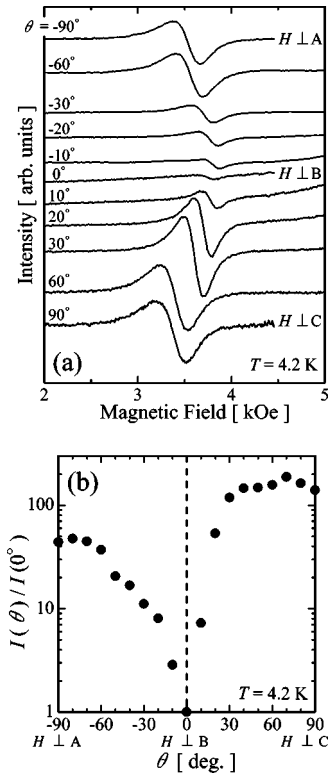

FIG. 9. (a) The angular dependence of the spectra of the half-field line observed at 4.2 K. The line seems to disappear when θ approaches 0°. (b) The angular dependence of the absorption intensity of the half-field line observed at 4.2 K. The values of $I(\theta)/I(0°)$ are plotted, where $I(0°)$ is the intensity at $\theta=0°$.

the absence of an antisymmetric exchange interaction between the spins of these pairs of Cu. The values $\Delta H_{pp} \simeq 300-500$ Oe observed at 295 K are explained when the magnetic dipole–dipole interaction, $\mathcal{H}'_{DD}$, and the anisotropic exchange interaction, $\mathcal{H}'_{AE}=\Sigma_i \mathbf{S}_i \cdot \tilde{\mathbf{A}}_{ii+1} \cdot \mathbf{S}_{i+1}$, are considered as perturbation terms that cause line broadening. To estimate the linewidth ΔH, the exchange-narrowing formula $\Delta H \simeq \hbar^2 M_2 / g\mu_B |J|$ was used, where M_2 is the second moment of the respective perturbation terms. The second moment due to $\mathcal{H}'_{AE}$ was calculated using a conventional approximate relation $|\tilde{\mathbf{A}}_{ii+1}| \equiv |A| \simeq |(\Delta g/g)^2 J|$ (where $\Delta g = g-2$).

In an ideal one-dimensional Heisenberg antiferromagnet (1DHAF), divergent behavior of a $\Delta H_{pp}(T)$ and a shift of $H_{res}(T)$ over the short-range ordering region are expected when $\mathcal{H}'_{DD}$ and $\mathcal{H}'_{AE}$ are origins of line broadening. Moreover, a diffusion process in the spin relaxation is expected to cause a non-Lorentzian line shape at high temperatures. The expectations for $\Delta H_{pp}(T)$ and $H_{res}(T)$ are satisfied; as shown in Figs. 5(a), 5(b), and 6(a), $\Delta H_{pp}(T)$ surely increases and $H_{res}(T)$ shifts when T approaches 10 K, i.e., when the short-range order develops. The gradual decrease in $\Delta H_{pp}(T)$ with decreasing temperature observed above 50 K is commonly seen in low-dimensional Cu^{2+} antiferromagnets in which $\mathcal{H}'_{DD}+\mathcal{H}'_{AE}$ causes line broadening. To explain such a decrease in $\Delta H_{pp}(T)$ over the temperature region where the short-range order is absent or very weak , we must take spin-phonon couplings into account, but this is not a subject of interest here.

Another experimental result, i.e., the observed Lorentzian line shape, is against the expectation for an ideal 1DHAF. Considering the established fact that a XY-like anisotropy does not violate the spin diffusion effect, whereas an Ising-type anisotropy, however weak it may be, destroys the effect of the diffusion process, we think that $\mathcal{H}'_{DD}+\mathcal{H}'_{AE}$ in this compound probably produces an Ising-type anisotropy field because the spin arrangement in this compound is unlikely to cause an XY-like anisotropy field. The Ising-type anisotropy wipes out the diffusion process, and this results in the Lorentzian line shape. As we have explained, the perturbation terms that cause the line broadening in the cause of this compound are $\mathcal{H}'_{DD}+\mathcal{H}'_{AE}$. The absence of an antisymmetric exchange interaction is important when the EPR data obtained at high frequencies and at high magnetic fields are analyzed, and this will be reported elsewhere.[8]

B. Below 10 K; formation of the Haldane state with $S=1$

Development of the magnetic short-range order in this compound means increasing numbers of pairs of ferromagnetically coupled spins. Each pair of spins is regarded as a spin with $S=1$. As a result, the singlet–triplet energy gap Δ is created. When $T \ll \Delta/k$, most of the spins occupy the singlet ground state, but the probability of occupation of the triplet state increases with increasing temperature. When H is applied, the threefold degeneracy of the triplet state is removed, and EPR absorption lines that correspond to the transitions of $\Delta S_z = \pm 1$ among the three levels of the triplet state, i.e., $S_z = 1,0,-1$, are expected. The expected EPR lines, if they are observed, will decrease in intensity with decreasing T because the population of spins in the triplet state decreases when T approaches 0 K.

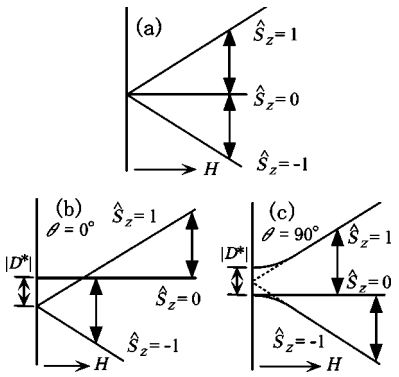

FIG. 10. The energy schemes of the triplet state (a) with threefold degeneracy, (b) assuming $D^*<0$ for $\theta=0°$, and (c) for 90°.

In the energy scheme in which the triplet state is degenerated at $H=0$, the two lines cannot be expected, as shown in Fig. 10(a). The appearance of the two lines below 10 K indicates that the threefold degeneracy of the triplet state at $H=0$ is removed for some reason. In magnetic compounds with $S=1$ such as NENP which is a representative Haldane system with Ni^{2+} ions, a single ion anisotropy DS_z^2 removes the threefold degeneracy at $H=0$. To confirm the energy scheme of the nondegenerate triplet state in NENP, several experimental[9–12] and theoretical[13–15] investigations of ESR were reported.

In the cause of $IPACuCl_3$, however, a single ion anisotropy term is absent because $S=1/2$. From the analyses of the crystal symmetry and the EPR lines observed above 10 K in $IPACuCl_3$, as mentioned earlier, an antisymmetric exchange interaction is absent. Moreover, if this interaction exists, the forbidden transition from the singlet state to the triplet state will be allowed. The absorption line corresponding to this transition, however, was not detected in ESR experiments performed at frequencies over 77–540 GHz under H up to 20 T.[8] Therefore, the interactions that act as anisotropy terms are $\mathcal{H}'_{DD}$ and $\mathcal{H}'_{AE}$ between the ferromagnetically coupled two spins.

We thought that $\mathcal{H}'_{DD}+\mathcal{H}'_{AE}$ should fill the role of a single ion anisotropy term over the temperature region where ferromagnetically coupled spins behave as a spin with $S=1$ and then form the Haldane state. Hereafter, a pair of spins is expressed as $\hat{\mathbf{S}} \equiv \mathbf{S}_1+\mathbf{S}_2$. The anisotropy terms $\mathcal{H}'_{DD}$ and $\mathcal{H}'_{AE}$ between $\mathbf{S}_1$ and $\mathbf{S}_2$ where $S=1/2$ serve as a substitute for a single ion anisotropy $D^*[\hat{S}_z^2-\hat{S}(\hat{S}+1)/3]$ with $\hat{S}=1$, as explained in the Appendix, where it is shown that $\mathcal{H}'_{DD}$ and $\mathcal{H}'_{AE}$ determined between ferromagnetically coupled two spins can both be treated similarly. As a result, the energy levels of the Zeeman interaction $g\mu_B \hat{\mathbf{S}} \cdot \mathbf{H}$ for $\hat{S}_z=+1,0,-1$ are modified by $\mathcal{H}'_{DD}$ and $\mathcal{H}'_{AE}$ between ferromagnetically coupled two spins. If the Zeeman energy is much stronger than that of $\mathcal{H}'_{DD}+\mathcal{H}'_{AE}$, the effects of the nondiagonal elements shown in Table II can be neglected when we discuss the energy levels of the $\hat{S}=1$ and $\hat{S}=0$ states. Therefore, these energy levels are expressed as

$$E_{1,1}=\Delta+g(\theta)\mu_B H-\frac{D^*}{6}(1-3\cos^2\theta),$$

$$E_{1,0}=\Delta+\frac{D^*}{3}(1-3\cos^2\theta),$$

$$E_{1,-1}=\Delta-g(\theta)\mu_B H-\frac{D^*}{6}(1-3\cos^2\theta), \tag{3.1}$$

$$E_{0,0}=0,$$

where $E_{l,m}$ is the energy of the $|\hat{S}=l,\hat{S}_z=m\rangle$ state and the anisotropy field is $D^*\equiv-3g^2\mu_B^2/(2r^3)-3A/2$, as explained in detail in the Appendix. As Eq. (3.1) indicates, the threefold degeneracy at $H=0$ is removed by $D^*[\hat{S}_z^2-\hat{S}(\hat{S}+1)/3]$. The energies that correspond to the $\Delta\hat{S}_z=\pm1$ transitions between the energy levels of the triplet state are

$$E_{1,1}-E_{1,0}=g(\theta)\mu_B H-\frac{D^*}{2}(1-3\cos^2\theta),$$

$$E_{1,0}-E_{1,-1}=g(\theta)\mu_B H+\frac{D^*}{2}(1-3\cos^2\theta). \tag{3.2}$$

On the basis of the assumption $D^*<0$, the energy schemes at $\theta=0°$ and 90° given by Eq. (3.1) are shown in Figs. 10(b) and 10(c), respectively. Recently, $D^*<0$ has been determined from ESR measurements at high frequencies up to 540 GHz.[8] To obtain Eqs. (3.1) and (3.2), $\hat{S}=1$ and $\hat{S}_z=1,0,-1$ are used in $D^*[\hat{S}_z^2-\hat{S}(\hat{S}+1)/3]$. The gradual shift of H_{res} of the two lines to the opposite sides with decreasing temperature, as shown in Fig. 6(b), is due to growth of the $D^*[\hat{S}_z^2-\hat{S}(\hat{S}+1)/3]$ term with decreasing temperature below 10 K.

The angular dependence of H_{res} of the two lines observed at 4.2 K, as shown in Fig. 7, well fits the curves $H_{res}\simeq a\pm b(1-3\cos^2\theta)$. This angular dependence coincides with Eq. (3.2). From the coincidence between the experimental results and the theoretical curves, one finds that $\theta=0°$ corresponds to $H\perp B$ plane, where θ is the angle between H and the bonding line of the two spins. Fitting Eq. (3.2) to the experimental results shown in Fig. 7, we obtain $|D^*|/g\mu_B\simeq2.2$ kOe at 4.2 K. This value roughly agrees with the calculated one $D^*\equiv-3g^2\mu_B^2/(2r^3)-3A/2$, i.e., $-3g^2\mu_B^2/(2r^3)=-0.7$ kOe and $-3|A|/2\simeq-3|(\Delta g/g)^2J_F|/2=-2.6$ kOe, where $r=3.5$ Å and $g=2.14$ is the averaged value of g_A, g_B, and g_C. Consequently, the anisotropy field D^* can be explained by $\mathcal{H}'_{DD}+\mathcal{H}'_{AE}$, though the sign of A is uncertain.

As can be seen in Table II, the three $|1,1\rangle$, $|1,0\rangle$, and $|1,-1\rangle$ states are not eigenstates because the nondiagonal elements are not 0. Hence, the transitions between $|1,1\rangle$ and $|1,-1\rangle$, i.e., the $\Delta\hat{S}_z=\pm2$ transition, becomes allowed, and the transition yields an absorption line at a frequency that corresponds to

$$E_{1,1}-E_{1,-1}=2g(\theta)\mu_B H. \tag{3.3}$$

That is the reason for the appearance of the half-field line. The observed weak angular dependence of the resonance field of the half-field line is due to the change in the g value with θ, i.e., $g(\theta)$. At extremely high fields, the nondiagonal elements shown in Table II are regarded as 0 compared with the Zeeman energy, so the half-field line disappears, as we have already confirmed by EPR experiments above 77 GHz.[8]

The origin of the two lines as well as the half-field line has been clarified, as explained above. The absorption intensity of each of the two lines monotonically decreases, as can be seen Fig. 8. Moreover, the intensity of the half-field line depends on the direction of H, as shown in Fig. 9(b). We now discuss why such phenomena occur. The ΔH_{pp} of the two lines decreases with decreasing T because the thermal fluctuation of spins becomes weak.

The temperature dependence of the absorption intensity which corresponds to the $\Delta S_z=\pm1$ transition observed in NENP was well explained by examining the population of spins in the triplet state.[11] Following the method displayed in Ref. 11, we calculate the temperature dependence of the absorption intensity in $IPACuCl_3$. The sum of the absorption intensities of the two lines is estimated on the basis of the energy scheme given by Eq. (3.1). When $\theta=0°$, the energy levels given by Eq. (3.1) are re-expressed as

$$\epsilon_3=\Delta+g(0)\mu_B H_H+\frac{D^*}{3},$$

$$\epsilon_2=\Delta-\frac{2D^*}{3},$$

$$\epsilon_1=\Delta-g(0)\mu_B H_L+\frac{D^*}{3}, \tag{3.4}$$

$$\epsilon_0=0,$$

where H_H and H_L are the resonance fields of the two lines that appear at higher and lower fields, respectively. The sum of absorption intensities I of the two lines that correspond to $\epsilon_1-\epsilon_2$ and $\epsilon_2-\epsilon_3$ are given by

$$I\propto\frac{(e^{-\epsilon_1/kT}-e^{-\epsilon_2/kT})+(e^{-\epsilon_2/kT}-e^{-\epsilon_3/kT})}{\sum_{i=0}^{3}e^{-\epsilon_i/kT}}. \tag{3.5}$$

Applying $D^*/g(0)\mu_B=-2.2$ kOe, $H_H=10.7$ kOe, $H_L=6.3$ kOe, $g(0)=2.06$, and $\Delta/k=17.5$ K, we obtain the curve shown in Fig. 8 by a solid line. In the calculation, the T dependence of D^* is neglected because $|D^*|\ll\Delta$. As can be seen in Fig. 8, the calculated curve and the experimental results do not coincide. At present, we have no idea how to explain the disagreement between the experimental result and the calculated result.

The angular dependence of the absorption intensity of the half-field line is next discussed. As can be seen in Figs. 9(a) and 9(b), the half-field line disappears at $\theta=0°$, and its intensity increases when θ approaches 90°. Since the half-field line is due to the transition between $|1,-1\rangle$ and $|1,1\rangle$, its intensity is closely correlated with the matrix element $\langle1,-1|\mathcal{H}'_{DD}+\mathcal{H}'_{AE}|1,1\rangle\propto\sin^2\theta$, given in Table II. Consequently, the absorption intensity should be 0 at $\theta=0°$ and should increase when θ increases to 90°, which agrees quali-

TABLE I. The energy matrix of two spins with $S=1/2$ for the dipole–dipole interaction and the anisotropic exchange interaction. The coefficients in the table are $C_0=g^2\mu_B^2/(4r^3)+A/4$, $C_1=g^2\mu_B^2e^{-i\phi}/(4r^3)+A/4$, $C_{-1}=g^2\mu_B^2e^{+i\phi}/(4r^3)+A/4$, $C_2=g^2\mu_B^2e^{-2i\phi}/(4r^3)+A/4$, and $C_{-2}=g^2\mu_B^2e^{+2i\phi}/(4r^3)+A/4$, respectively.

$\langle S_1,S_1^z\vert\langle S_2^z,S_2^z\vert \times\vert S_1,S_1^z\rangle\vert S_2,S_2^z\rangle$	$\vert 1/2,1/2\rangle \times\vert 1/2,1/2\rangle$	$\vert 1/2,1/2\rangle \times\vert 1/2,-1/2\rangle$	$\vert 1/2,-1/2\rangle \times\vert 1/2,1/2\rangle$	$\vert 1/2,-1/2\rangle \times\vert 1/2,-1/2\rangle$
$\langle 1/2,1/2\vert\langle 1/2,1/2\vert$	$C_0(1-3\cos^2\theta)$	$-3C_1\sin\theta\cos\theta$	$-3C_1\sin\theta\cos\theta$	$-3C_2\sin^2\theta$
$\langle 1/2,1/2\vert\langle 1/2,-1/2\vert$	$-3C_{-1}\sin\theta\cos\theta$	$-C_0(1-3\cos^2\theta)$	$-C_0(1-3\cos^2\theta)$	$3C_1\sin\theta\cos\theta$
$\langle 1/2,-1/2\vert\langle 1/2,1/2\vert$	$-3C_{-1}\sin\theta\cos\theta$	$-C_0(1-3\cos^2\theta)$	$-C_0(1-3\cos^2\theta)$	$3C_1\sin\theta\cos\theta$
$\langle 1/2,-1/2\vert\langle 1/2,-1/2\vert$	$-3C_{-2}\sin^2\theta$	$3C_{-1}\sin\theta\cos\theta$	$3C_{-1}\sin\theta\cos\theta$	$C_0(1-3\cos^2\theta)$

tatively with the experimental results. The difference in intensities between $H\perp$ A plane and $H\perp$ C plane, both of which correspond to $\theta=90°$, is a result of the rough treatment of the tensor $\tilde{\mathbf{A}}_{ii+1}$ in $\mathcal{H}'_{AE}$. That is, the assumption $\tilde{\mathbf{A}}_{12}\equiv(A,A,-2A)$ is not adequate for $IPACuCl_3$ because the spin arrangement of this compound is not tetragonal, and therefore discussion of Fig. 9(b) in quantitative terms is hard.

IV. CONCLUSION

The drastic change in the EPR spectrum of $IPACuCl_3$ around 10 K was found to be attributable to the crossover from the $S=1/2$ state to the Haldane state with $S=1$. The dipole–dipole interaction and the anisotropic exchange interaction between ferromagnetically coupled two spins act as a fictitious single ion anisotropy. The fictitious single ion anisotropy removes the threefold degeneracy of the triplet state at $H=0$, and consequently yields the two absorption lines that are observed below 10 K.

As can be seen in Table II, the matrix elements between the $\langle 0,0\vert$ state and the three $\vert 1,1\rangle$, $\vert 1,0\rangle$, and $\vert 1,-1\rangle$ states are 0. Thus an absorption line that corresponds to the transition from the singlet state to the triplet state cannot be expected. From the high frequency ESR experiments,[8] we confirmed the absence of such a forbidden line. These results will be reported elsewhere.

ACKNOWLEDGMENTS

The authors thank K. Katsumata, M. Hagiwara, K. Hida, T. Kubo, H. Tanaka, T. Sakai, and S. Kokado for useful comments and discussion. This research was supported in part by a Grant-in-Aid for Scientific Research from the Ministry of Education, Sciences, Sports and Culture. One of the authors (H.M.) was supported by the Japan Society for the Promotion of Science for Young Scientists.

APPENDIX

At low temperatures, ferromagnetically coupled two spins in $IPACuCl_3$, $\mathbf{S}_1$ and $\mathbf{S}_2$, with $S_1=S_2=1/2$, turn into a spin $\hat{\mathbf{S}}(\equiv\mathbf{S}_1+\mathbf{S}_2)$ with $\hat{S}=1$. We explain the formation of the fictitious single ion anisotropy $D^*[\hat{S}_z^2-\hat{S}(\hat{S}+1)/3]$ of a spin $\hat{\mathbf{S}}$ from the dipole–dipole interaction and the anisotropic exchange interaction between $\mathbf{S}_1$ and $\mathbf{S}_2$. The Hamiltonian of the dipole–dipole interaction $\mathcal{H}'_{DD}$ and the anisotropic exchange interaction $\mathcal{H}'_{AE}$ for the two spins $\mathbf{S}_1$ and $\mathbf{S}_2$ are given by

$$\mathcal{H}'_{DD}=\frac{g^2\mu_B^2}{r^3}\left[\mathbf{S}_1\cdot\mathbf{S}_2-\frac{3(\mathbf{S}_1\cdot\mathbf{r})(\mathbf{S}_2\cdot\mathbf{r})}{r^2}\right], \tag{A1}$$

$$\mathcal{H}_{AE}=\mathbf{S}_1\cdot\tilde{\mathbf{A}}_{12}\cdot\mathbf{S}_2. \tag{A2}$$

To simplify the discussion, we tentatively assume a tetragonal crystal structure and then the tensor $\tilde{\mathbf{A}}_{12}$ consists of the diagonal part, i.e., $\tilde{\mathbf{A}}_{12}=(A_{12}^{XX},A_{12}^{YY},A_{12}^{ZZ})\equiv(A,A,-2A)$, where the coordinates $[X,Y,Z]$ are fixed on the assumed tetragonal axes. Equations (A1) and (A2) are combined into one and are expressed on a coordinate system $[x,y,z]$, where $H//z$ axis as

$$\mathcal{H}'_{DD}+\mathcal{H}'_{AE}=G_0+G_1+G_{-1}+G_2+G_{-2}, \tag{A3}$$

in which

$$G_0=S_1^zS_2^z(\Gamma+A)(1-3\cos^2\theta)-\tfrac{1}{4}(S_1^+S_2^-+S_1^-S_2^+)(\Gamma+A)\times(1-3\cos^2\theta),$$

$$G_1=-\tfrac{3}{2}(S_1^+S_2^z+S_1^zS_2^+)(\Gamma e^{-i\phi}+A)\sin\theta\cos\theta,$$

$$G_{-1}=-\tfrac{3}{2}(S_1^-S_2^z+S_1^zS_2^-)(\Gamma e^{+i\phi}+A)\sin\theta\cos\theta,$$

TABLE II. The energy matrix in the case where $\hat{S}=1$. The coefficients C_0, C_1, C_{-1}, C_2, and C_{-2} are the same as given in Table I.

$\langle\hat{S},\hat{S}_z\vert\hat{S},\hat{S}_z\rangle$	$\vert 1,1\rangle$	$\vert 1,0\rangle$	$\vert 1,-1\rangle$	$\vert 0,0\rangle$
$\langle 1,1\vert$	$C_0(1-3\cos^2\theta)$	$-3\sqrt{2}C_1\sin\theta\cos\theta$	$-3C_2\sin^2\theta$	0
$\langle 1,0\vert$	$-3\sqrt{2}C_{-1}\sin\theta\cos\theta$	$-2C_0(1-3\cos^2\theta)$	$3C_1\sqrt{2}\sin\theta\cos\theta$	0
$\langle 1,-1\vert$	$-3C_{-2}\sin^2\theta$	$3\sqrt{2}C_{-1}\sin\theta\cos\theta$	$C_0(1-3\cos^2\theta)$	0
$\langle 0,0\vert$	0	0	0	0

$$G_2 = -\tfrac{3}{4} S_1^+ S_2^+ (\Gamma e^{-2i\phi} + A)\sin^2\theta,$$

$$G_{-2} = -\tfrac{3}{4} S_1^- S_2^- (\Gamma e^{+2i\phi} + A)\sin^2\theta,$$

where $\Gamma \equiv g^2\mu_B^2/r^3$, while θ is the polar angle and ϕ is the azimuthal angle of $\mathbf{r}$ with respect to the direction of H. The energy matrix of the two spins with $S=1/2$ is given in Table I.

The singlet and the triplet state of $\hat{\mathbf{S}}$ are expressed as linear combinations of $|S_1, S_1^z\rangle$ and $|S_2, S_2^z\rangle$. They are

$$|\hat{S}, \hat{S}_z\rangle : |S_1, S_1^z\rangle |S_2, S_2^z\rangle,$$

$$|1,1\rangle : |1/2,1/2\rangle |1/2,1/2\rangle,$$

$$|1,0\rangle : \frac{1}{\sqrt{2}}(|1/2,1/2\rangle |1/2,-1/2\rangle + |1/2,-1/2\rangle |1/2,1/2\rangle),$$

$$|1,-1\rangle : |1/2,-1/2\rangle |1/2,-1/2\rangle, \tag{A4}$$

$$|0,0\rangle : \frac{1}{\sqrt{2}}(|1/2,1/2\rangle |1/2,-1/2\rangle - |1/2,-1/2\rangle |1/2,1/2\rangle).$$

Consequently, the energy matrix of $\hat{S}=1$ can be calculated using the result given in Table I, and is shown in Table II.

*Email address: manaka@physics.s.chiba-u.ac.jp

[1] F.D.M. Haldane, Phys. Lett. A **93**, 464 (1983); Phys. Rev. Lett. **50**, 1153 (1983).
[2] K. Hida, Phys. Rev. B **46**, 8268 (1992); J. Phys. Soc. Jpn. **62**, 1463 (1993).
[3] M. Yamanaka, Y. Hatsugai, and M. Kohmoto, Phys. Rev. B **48**, 9555 (1993).
[4] H. Manaka, I. Yamada, and K. Yamaguchi, J. Phys. Soc. Jpn. **66**, 564 (1997).
[5] H. Manaka, I. Yamada, N.V. Mushnikov, and T. Goto, J. Phys. Soc. Jpn. **69**, 675 (2000).
[6] H. Manaka, I. Yamada, Z. Honda, H. Aruga Katori, and K. Katsumata, J. Phys. Soc. Jpn. **67**, 3913 (1998).
[7] S.A. Roberts, D.R. Bloomquist, R.D. Willett, and H.W. Dodgen, J. Am. Chem. Soc. **103**, 2603 (1981).
[8] H. Manaka, I. Yamada, M. Hagiwara, and M. Tokunaga (unpublished).
[9] M. Date and K. Kindo, Phys. Rev. Lett. **65**, 1659 (1990).
[10] W. Lu, J. Tuchendler, M. von Ortenberg, and J.P. Renard, Phys. Rev. Lett. **67**, 3716 (1991).
[11] L.C. Brunel, T.M. Brill, I. Zaliznyak, J.P. Boucher, and J.P. Renard, Phys. Rev. Lett. **69**, 1699 (1992).
[12] M. Sieling, W. Palme, and B. Lüthi, Z. Phys. B **96**, 297 (1995).
[13] I. Affleck, Phys. Rev. B **46**, 9002 (1992).
[14] T. Sakai and H. Shiba, J. Phys. Soc. Jpn. **63**, 867 (1994).
[15] J. Sagi and I. Affleck, Phys. Rev. B **53**, 9188 (1996).